

Crystal Structure of the Human Papillomavirus Type 18 E2 Activation Domain

Seth F. Harris and Michael R. Botchan*

The papillomavirus E2 protein regulates viral transcription and DNA replication through interactions with cellular and viral proteins. The amino-terminal activation domain, which represents a protein class whose structural themes are poorly understood, contains key residues that mediate these functional contacts. The crystal structure of a protease-resistant core of the human papillomavirus type 18 E2 activation domain reveals a novel fold creating a cashew-shaped form with a glutamine-rich α helix packed against a β -sheet framework. The protein surface shows extensive overlap of determinants for replication and transcription. The structure broadens the concept of activators to include proteins with potentially malleable, but certainly ordered, structures.

protein colocalize with host cell chromosomes during mitosis, dependent on an intact E2 AD and phosphorylation sites within the hinge (11).

In this rich biological context, further understanding of E2 seemed poised to benefit from a structural study. We used limited proteolysis to identify an NH₂-terminal core domain (amino acids 1 through 207) of BPV1 E2. Diffracting crystals of this construct were difficult to obtain, but it served as a guide for similar proteolysis experiments on the HPV16 and HPV18 E2 proteins that each produced two AD fragments. Crystals were grown of both HPV18 constructs (amino acids 1 through 215 and 66 through 215) (12). Selenomethionine-substituted crystals permitted phase determination by multiwavelength anomalous diffraction (MAD) techniques (13). The resulting experimental maps allowed the construction of a model including all but seven residues of the shorter E2 AD core (Table 1).

The E2 AD is characterized by a cashew shape of 55 Å by 40 Å by 30 Å, with a concave cleft on one side of the protein and ridges on the opposite surface (Fig. 1). Its fold is novel as gauged by three-dimensional structure comparisons using DALI (14). A 17-residue NH₂-terminal helix and a subsequent distorted helical loop pack against a β -sheet framework built of antiparallel strands. The first two sheets form a larger arc that cradles the smaller, more bent sheet (Fig. 1B). There is an intricate layering of β strands that are relatively bowed or briefly

Papillomaviruses maintain latency in dividing stem cells of various epithelial tissues, replicating as extrachromosomal plasmids. Several of the high-risk variants of the human papillomavirus (HPV), including HPV18, are particularly associated with cervical cancer and other intraepithelial neoplasias (1). Viral protein levels, and ultimately the virus life cycle, are regulated by various forms of the viral transcription factor E2 and their interaction with the viral helicase E1. The ~45-kD E2 proteins characterized from numerous human and animal serotypes share a common organization of two modular domains. An NH₂-terminal activation domain (AD) of ~200 amino acids and a COOH-terminal DNA binding domain (DBD) of 100 amino acids in length are joined by a flexible hinge region. The E2 DBD dimerizes to form a β barrel with flanking recognition helices positioned in the major grooves of the DNA binding site (2). In contrast, the E2 AD, like transcription ADs in general, has remained enigmatic from a structural standpoint. Although this has fostered models based on induced fit with interacting partners (3), the extensive sensitivity of the E2 protein to point mutations over the entire AD is suggestive of a discrete disruptable structure, as confirmed by our work.

E2 activates viral replication through cooperative binding with the viral initiator protein E1 to the origin of DNA replication (4), ultimately resulting in functional E1 hexamers (5). E2 is also a central regulator of viral transcription. It interacts with basal transcription factors, including TATA-binding protein, TFIIB, and human TAF_{II}70 (6, 7); proximal promoter binding proteins such as Sp1

(8); and other cellular factors such as AMF-1 (9), which positively affect E2's transcriptional activation. Which of these many interactions are sufficient or necessary to achieve transcriptional activation is more ambiguous. These details are consistent with the idea that enhancer binding proteins function as transcriptional activators by using specific protein-protein contacts to link components of the general transcription machinery to a promoter, with the goal of recruiting RNA polymerase (10). A third function of E2 is to aid in the faithful segregation of viral DNA. The bovine papillomavirus (BPV) genome and E2

Table 1. Crystallographic data, phasing, and refinement. The crystals are of space group *P6₃22*. Data were collected on beamline 5.0.2 at the ALS, LBNL, and beamline 1-5 at the SSRL. Indexing was performed with MOSFLM/SCALA (27, 28) or the HKL suite (29). Initial phases were determined with SOLVE (30), which located two of four possible selenium sites in the asymmetric unit, and phases were solvent-flattened (31) with DM (28, 32). The model was built with O (33). Further clarification of specific areas was aided by application of SOLVE to the ALS MAD data set, which identified all four selenium sites and unambiguously corrected a misregistration near the COOH-terminus of the protein fragment. Refinement was performed with CNS (34) initially using only experimental phases to 2.8 Å. Eventually, the 2.1 Å native data set was incorporated, and phases were calculated from all the data with SHARP (35). Water molecules were added during later stages of refinement. General data manipulations were performed with the CCP4 suite of crystallography software (28). rmsd, root mean square deviation; deg, degrees.

	Native (ALS)	MAD (ALS)	MAD (SSRL)
Unit cell (Å)			
<i>a</i> = <i>b</i>	76.18	76.46	76.70
<i>c</i>	158.20	158.31	158.67
Resolution (Å)	2.1	2.8	2.8
<i>R</i> _{sym} (%) [*]	5.2	19.1	10.8
Unique reflections	16,635	7,342	8,098
Observed reflections	135,695	174,510	222,327
Completeness (%)	99.4	99.6	99.7
Fold multiplicity	6	13	13
Geometry		Refinement	
rmsd bond lengths (Å)	0.007	FOM (SOLVE)	0.53
rmsd bond angles (deg)	1.2	FOM (DM)	0.77
Most favored phi-psi (%)	91.6	<i>R</i> _{cryst} (%) [†]	25.6
Additionally allowed (%)	7.6	<i>R</i> _{free} (%) [†]	29.6
Generously allowed (%)	0.8	Waters	144

^{*}*R*_{sym} = $\sum |I - \langle I \rangle| / \sum I$, where *I* is intensity. [†]*R* factor = $\sum |F_o - F_c| / \sum |F_o|$, where *F_o* and *F_c* are observed and calculated structure factors, respectively, and *R*_{free} is the cross-validation *R* factor calculated with 10% of the data omitted from refinement.

Department of Molecular and Cell Biology, University of California, Berkeley, CA 94720-3204, USA.

*To whom correspondence should be addressed. E-mail: mbotchan@uclink4.berkeley.edu

REPORTS

disrupted as they transition between alternate sheets. A similar break is imposed by a prominent Cys side chain in helical region 2, disjoining two helical turns. Flexible loops that connect the strands and helices are generally exposed at the edges of the protein.

The various E2 proteins average 30% amino acid sequence identity (Fig. 2). The proteins also show functional conservation, as combinations of intertypic E1 and E2 genes can complement each other for viral replication. Such cross-variant interaction has been achieved with HPV11, HPV16, and BPV1 in pairwise mixing of the respective E1 and E2 genes (15). Also, mutational analyses on BPV1, HPV16, and HPV31 E2 genes have shown consistent results: Many residues throughout the AD are important for both transcription and replication, compatible with the idea that surfaces for both biochemical activities are interleaved. However, in all three E2 types, two amino acid substitutions clearly separated these two capacities. Changing Ile⁷³ to Ala (Ile73Ala) destroyed transcriptional activation while leaving replication functions intact, whereas replacing Glu³⁹ with Ala (Glu39Ala) had the inverse phenotype (16–19). Together, these findings support the idea that the various E2 ADs share a common fold and mechanism of action.

We have therefore combined the results of the mutagenesis analyses with the HPV18 E2 AD structure to study if discrete surfaces cor-

relate with known E2 activities. As anticipated, conserved residues are frequently buried (Fig. 2). Given that many buried residues pack tightly in a hydrophobic core or participate in diverse ionic interactions, Ala substitutions at these positions would be expected to have destabilizing effects. Indeed, such mutations fre-

quently impact both replication and transcription. In several cases, the stability of the mutant proteins has been directly examined. Three BPV mutants in particular show low protein levels in cultured cells (Leu82Ala, Trp92Ala, and Lys112Ala) (16). Furthermore, purified Lys112Ala and Leu82Ala mutant E2 proteins

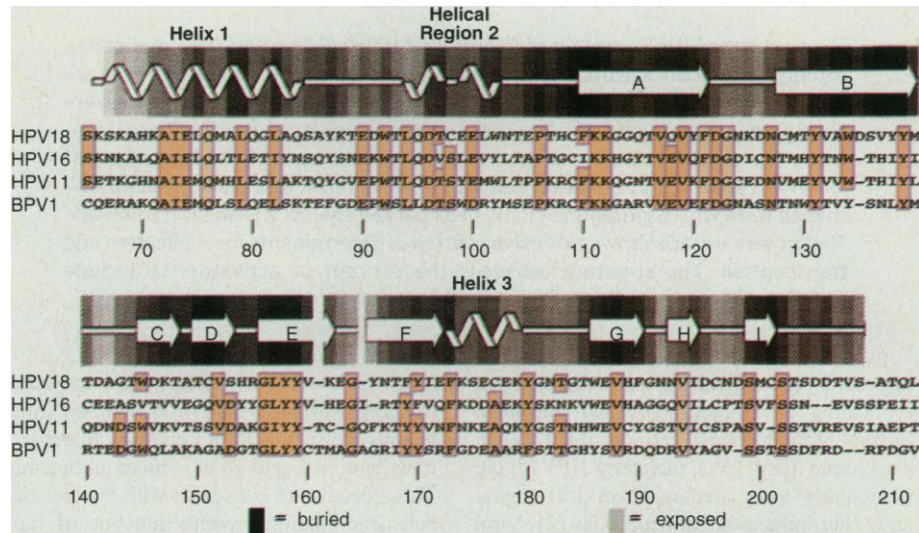


Fig. 2. Sequence alignment of four papillomavirus E2 proteins matched to the secondary structure, shaded by relative exposure of the backbone [PROCHECK (28)]. There is a qualitative correlation between more conserved regions (salmon shading) and buried positions (dark shading). Numbering is according to BPV convention.

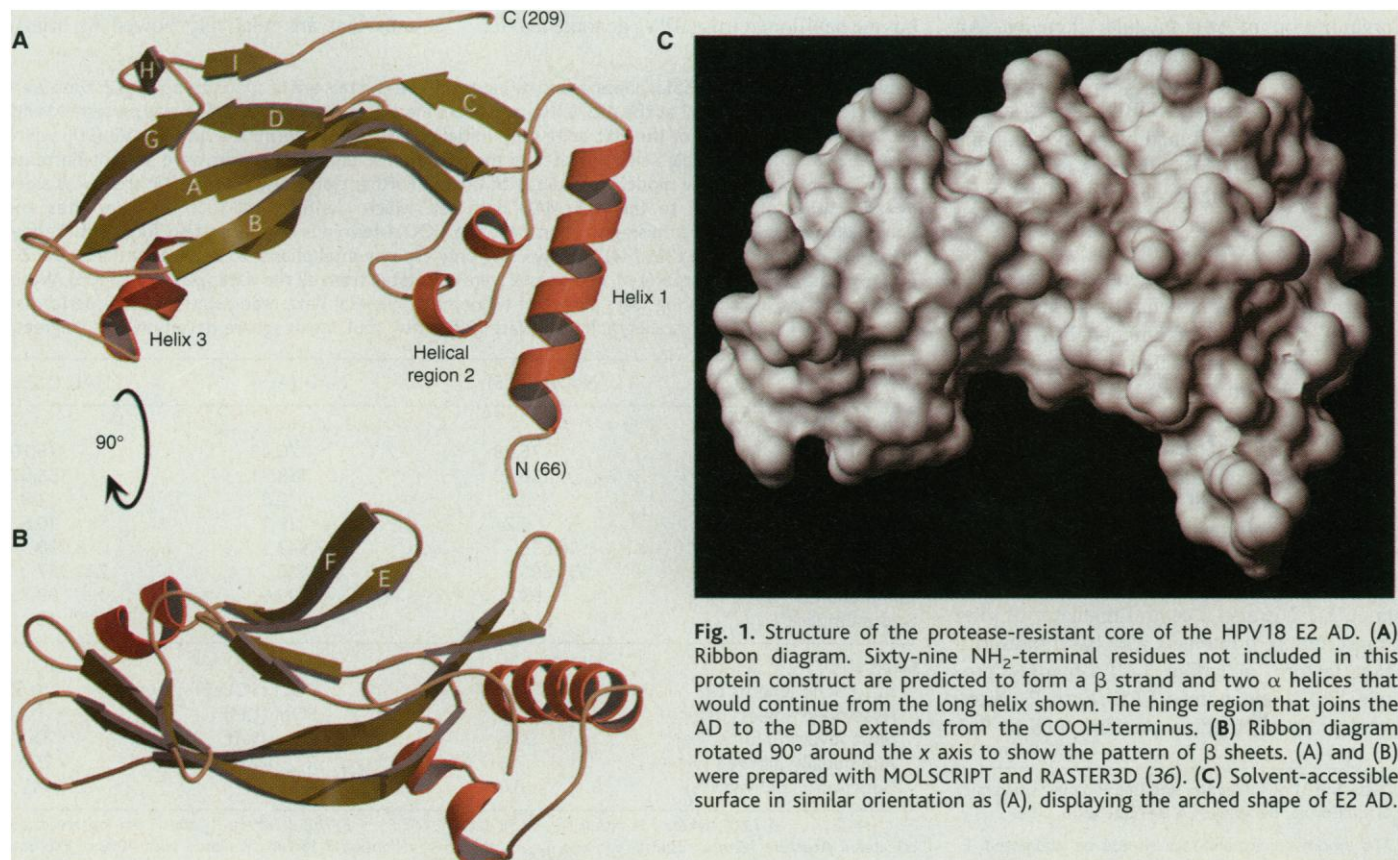


Fig. 1. Structure of the protease-resistant core of the HPV18 E2 AD. (A) Ribbon diagram. Sixty-nine NH₂-terminal residues not included in this protein construct are predicted to form a β strand and two α helices that would continue from the long helix shown. The hinge region that joins the AD to the DBD extends from the COOH-terminus. (B) Ribbon diagram rotated 90° around the x axis to show the pattern of β sheets. (A) and (B) were prepared with MOLSCRIPT and RASTER3D (36). (C) Solvent-accessible surface in similar orientation as (A), displaying the arched shape of E2 AD.

REPORTS

have a heightened sensitivity to proteolysis (20), which is consistent with a comprehensive loosening of the fold.

Tight packing in the HPV18 structure provides insight into these effects. For example, Lys¹¹² is involved in charge interactions with the acidic side chain of Glu⁹⁰ and the backbone carbonyl oxygen of Asp⁹¹. Conversion of this Lys to an Ala eliminates these ion pairs. Similarly, the hydrophobic environment around residues Trp⁹² and Leu⁸² would be sensitive to mutation at those positions (see Web Fig. 1, available at www.sciencemag.org/feature/data/

991001.shl). These points, illuminated by the structure, show how difficult it may be by simple loss-of-function assays to discern those residues of E2 that may be interacting specifically with other cellular or viral partners. With this structure, we can focus on candidate amino acids poised for intermolecular interactions, enabling exploration of less conserved features (Fig. 3A, right).

Examination of surface residues in light of the mutant phenotypes indicates that broad and clear zones of transcription function and replication function are not segregated on the

surface of the core (Fig. 3, B and C). Important amino acids for each of these functions are numerous and widely spaced. The striking overlap hints at mechanistic insights because most of the documented E2-interacting factors have a primary importance for either replication or transcription, but not both. Consequently, many of the surfaces that are utilized for both functions might compete for similarly structured targets in replication or transcription complexes.

Small patches of residues throughout the surface may in some cases be more critical for one activity or the other. A prominent cluster of mutants that preferentially affect replication lies on the inner edge of the main cavity, distal to the long NH₂-terminal helix (Fig. 3B). This well-conserved, exposed region encompasses residues Glu¹⁷⁵, Lys¹⁷⁸, and Tyr¹⁷⁹, which protrude from a shorter α helix. Also, Ile⁷³, although hydrophobic, is exposed on the long NH₂-terminal α helix and defines a distinctive surface that is more important for transcription than for replication.

Guided by the structure, we further explored the outside face of this helix, targeting three Gln residues just COOH-terminal to Ile⁷³ for Ala substitution (21) (Fig. 4). In transient cell-based functional assays (22), individual mutations show an increasing effect on transcription the closer they are to the NH₂-terminal region of the helix (that is, the vicinity of Ile⁷³). These mutants had modest or no effect on replication functions (Fig. 4). The pattern of these results, corroborated by analogous mutations made in BPV E2 (23), is consistent with this helix surface being important in transcriptional activation. We speculate that the hydrophobic Ile⁷³ helps in establishing transcriptionally important protein-protein interactions with further stabilization and specificity provided by the polar Gln⁷⁶. The prevalence of Gln in particular is reminiscent of the general class of Gln-rich ADs. This helical array may provide a template for the three-dimensional disposition of Gln's in their namesake activators.

The analysis of the NH₂-terminal α helix of E2 draws similarities with structural studies of the activator peptides from p53, cyclic adenosine 3',5'-monophosphate response element-binding protein (CREB), and VP16, all of which are believed to have a direct role in transcription (24). When examined as isolated peptides, they are disordered, but each is induced to form an amphipathic α helix by the hydrophobic surfaces on heterologous partner proteins. In the absence of an interacting partner, the corresponding E2 AD amphipathic helix is, in contrast, stabilized by the packing of its hydrophobic face against the β -sheet framework of E2 itself. Still, hydrophobic protrusions of Ile⁷³ and the nearby Met⁷⁷, alternately a Leu in many variants, remain

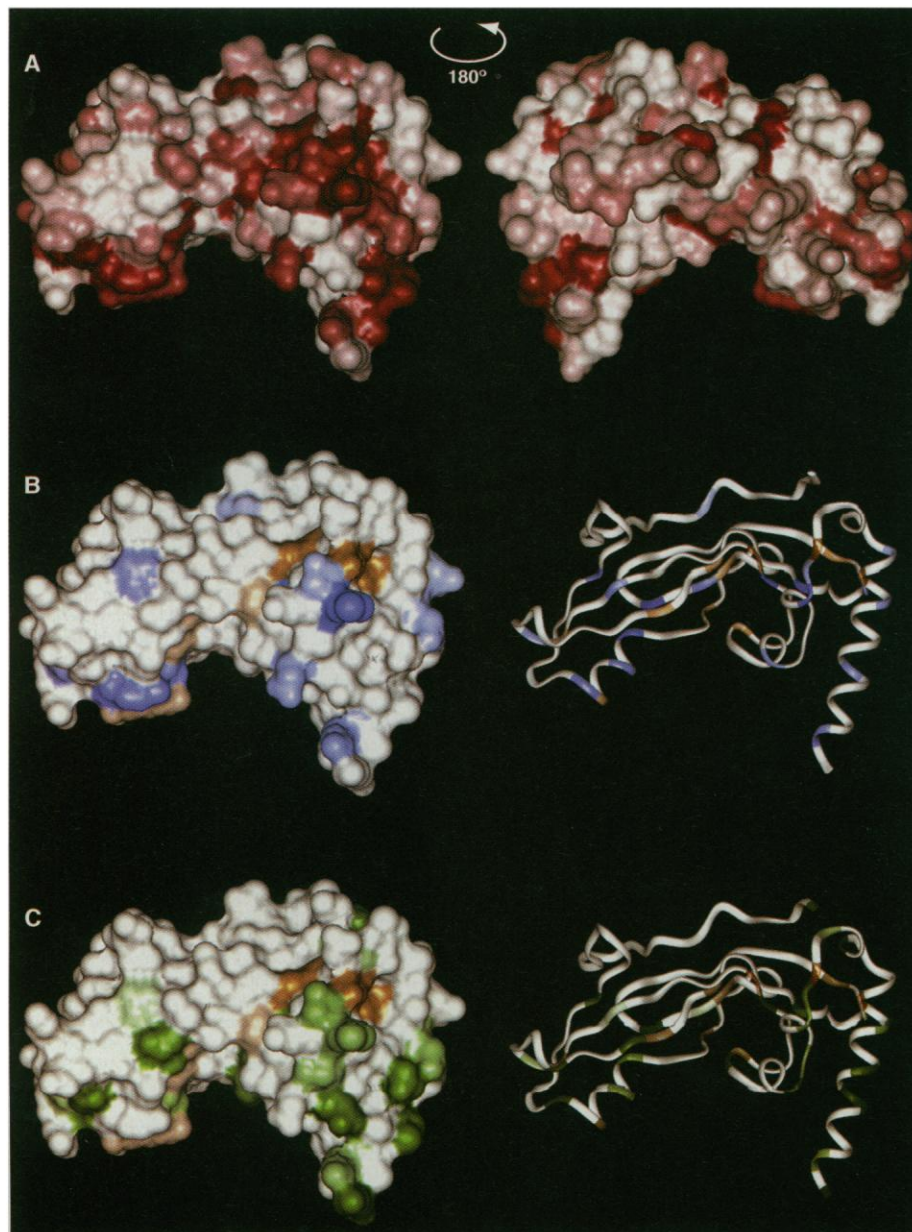
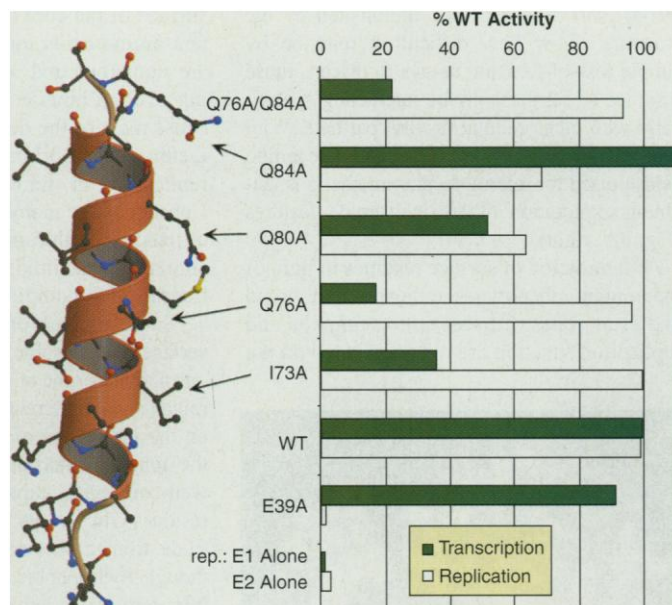


Fig. 3. Solvent-accessible surfaces and ribbon diagrams colored by conservation or disruption of biological function. This figure compiles data from five groups (16–19) and is therefore presented as a qualitative tool. (A) More conserved positions are deeper red. Fewer areas are both exposed and conserved on the back surface. (B) Residues whose mutation disrupts replication are blue, and those that substantially lower protein accumulation are colored putty. The accompanying ribbon diagram shows orientation and internal residues. (C) Similar views as above are colored by effect on transcription (green).

REPORTS

Fig. 4. The NH₂-terminal helix showing effects of Ala mutations on transcription and replication (22). Strongest effects on transcription occur for Ile73Ala (I73A) and Gln76Ala (Q76A), leaving replication at wild-type levels. Glu39Ala (E39A) shows truly diminished replication in the presence of both E1 and E2. Data has been normalized and expressed as a percentage of wild-type (WT) levels.



exposed and could help mediate strong and specific intermolecular contacts.

The diverse roles of E2 mandate that its structure, although discrete and ordered, accommodate requirements for high-affinity interactions with multiple specificities. These need not be conflicting obligations but rather may be achieved with a certain degree of flexibility. Suppleness at key joints could allow contact surfaces to adopt a large number of related, but clearly distinguishable, topologies. Several regions of E2 might provide such pliancy. Exposed loops have relatively high *B* factors and the poorest density, suggestive of multiple conformations in the crystal. A study has implicated Asn¹²⁷ that is in one such loop as important for interaction with TFIIB (6). Although well-ordered in this structure, conformational flexibility in a Pro¹⁰⁶-kinked loop, just COOH-terminal to the interrupted helical region 2, could allow it to regulate access to or modify the shape of the large concave cleft.

What evolutionary forces might distinguish E2 from other eukaryotic activators that seem to be less ordered when not in a complex? We speculate that E2's multiple functions and, in particular, its major role in replication may drive such constraints. E2's primary partner, the viral helicase E1, is suggested to interact with a relatively large surface of E2. This observation extends beyond the areas included in this structure, as peptides based on the E2 sequence around Glu³⁹ are able to block both replication and E1-E2 interaction (25), a correlation also noted in several other mutants (19). Ultimately, the breadth of such surface contacts may surpass that used specifically for transcription. E1 would therefore be expected to supply many of the structural constraints on the evolution of E2. This selective force is mirrored at the

genetic level, where the coding regions for E1 and E2 overlap slightly in alternate reading frames. As a corollary, the multiple surfaces on E2 involved in transcription may be necessitated by contact with several partners, each of which alone needs only a small surface. This describes a different pattern of constraints than that modeled for the E2-E1 interaction: a different set of evolutionary forces that may distinguish such multifunctional proteins from more dedicated peptides. Activators with extremely mosaic patternings of small interaction surfaces may be deconstrained to the point that structural analysis is indeed impossible outside of the context of interacting partners (26). It seems likely, however, that other eukaryotic enhancer binding proteins will have functional constraints similar to those of E2 and will therefore be amenable to structural studies that are independent of a more complex framework.

References and Notes

- F. X. Bosch et al., *J. Natl. Cancer Inst.* **87**, 796 (1995).
- R. S. Hegde, S. R. Grossman, L. A. Laimins, P. B. Sigler, *Nature* **359**, 505 (1992); H. Liang et al., *Biochemistry* **35**, 2095 (1996); R. S. Hegde and E. J. Androphy, *J. Mol. Biol.* **284**, 1479 (1998).
- A. D. Frankel and P. S. Kim, *Cell* **65**, 717 (1991); P. B. Sigler, *Nature* **333**, 210 (1988).
- J. Z. Lu, Y. N. Sun, R. C. Rose, W. Bonnez, D. J. McCance, *J. Virol.* **67**, 7131 (1993); I. J. Mohr et al., *Science* **250**, 1694 (1990); J. Sedman and A. Stenlund, *EMBO J.* **14**, 6218 (1995); Y. S. Seo, F. Muller, M. Lusk, J. Hurwitz, *Proc. Natl. Acad. Sci. U.S.A.* **90**, 702 (1993); M. G. Frattini and L. A. Laimins, *Virology* **204**, 799 (1994); L. Yang, R. Li, I. J. Mohr, R. Clark, M. R. Botchan, *Nature* **353**, 628 (1991).
- T. Sedman, J. Sedman, A. Stenlund, *J. Virol.* **71**, 2887 (1997); M. Lusk and E. Fontane, *Proc. Natl. Acad. Sci. U.S.A.* **88**, 6363 (1991); E. T. Fouts, X. Yu, E. H. Egelman, M. R. Botchan, *J. Biol. Chem.* **274**, 4447 (1999).
- J. M. Yao, D. E. Breiding, E. J. Androphy, *J. Virol.* **72**, 1013 (1998).
- J. D. Benson, R. Lawande, P. M. Howley, *ibid.* **71**, 8041 (1997); N. M. Rank and P. F. Lambert, *ibid.* **69**, 6323 (1995).

- R. Li, J. D. Knight, S. P. Jackson, R. Tjian, M. R. Botchan, *Cell* **65**, 493 (1991); B. A. Spalholz, S. B. Vande Pol, P. M. Howley, *J. Virol.* **65**, 743 (1991).
- D. E. Breiding et al., *Mol. Cell. Biol.* **17**, 7208 (1997).
- M. Ptashne and A. Gann, *Nature* **386**, 569 (1997); R. Tjian and T. Maniatis, *Cell* **77**, 5 (1994).
- C. W. Lehman and M. R. Botchan, *Proc. Natl. Acad. Sci. U.S.A.* **95**, 4338 (1998); M. H. Skiadopoulos and A. A. McBride, *J. Virol.* **72**, 2079 (1998).
- E2 constructs were proteolyzed by elastase (Roche, Indianapolis, IN) at a ratio by weight of 1:100 protease:E2 for 10 to 120 min. Mass spectrometry and NH₂-terminal sequencing identified protease-resistant end points. Purification and crystallization details are available at www.sciencemag.org/feature/data/991001.shl
- W. A. Hendrickson, *Science* **254**, 51 (1991).
- L. Holm and C. Sander, *J. Mol. Biol.* **233**, 123 (1993).
- N. Zou, J. S. Liu, S. R. Kuo, T. R. Broker, L. T. Chow, *J. Virol.* **72**, 3436 (1998); C. M. Chiang et al., *Proc. Natl. Acad. Sci. U.S.A.* **89**, 5799 (1992).
- M. K. Ferguson and M. R. Botchan, *J. Virol.* **70**, 4193 (1996).
- A. Abroi, R. Kurg, M. Ustav, *ibid.*, p. 6169; D. E. Breiding, M. J. Grossel, E. J. Androphy, *Virology* **221**, 34 (1996); J. L. Brokaw, M. Blanco, A. A. McBride, *J. Virol.* **70**, 23 (1996).
- F. Stubenrauch, A. M. Colbert, L. A. Laimins, *J. Virol.* **72**, 8115 (1998).
- H. Sakai, T. Yasugi, J. D. Benson, J. J. Dowhanick, P. M. Howley, *ibid.* **70**, 1602 (1996).
- M. K. Ferguson, S. F. Harris, M. R. Botchan, unpublished observations.
- Mutants were generated with a QuickChange kit (Stratagene) and verified by sequencing.
- For transcription, we averaged three to five transfections in C33A cells using 0.3 to 1 μg of E2 expression vector, 0.5 μg of reporter plasmid 6x E2SVLuc [kindly provided by L. A. Laimins (18)], and 30 μg of carrier DNA. For replication, we averaged two transfections of two time points each, using 2 μg of E2 expression vector, 1 to 3 μg of E1 expression vector [M. Remm, A. Remm, M. Ustav, *J. Virol.* **73**, 3062 (1999)], 1 μg of the origin-containing template (nucleotides 7800 to 118 of the HPV18 genome), and 30 μg of carrier DNA.
- S. F. Harris and M. R. Botchan, data not shown.
- I. Radhakrishnan et al., *Cell* **91**, 741 (1997); P. H. Kussie et al., *Science* **274**, 948 (1996); M. Uesugi, O. Nyanguile, H. Lu, A. J. Levine, G. L. Verdine, *ibid.* **277**, 1310 (1997).
- H. Kasukawa, P. M. Howley, J. D. Benson, *J. Virol.* **72**, 8166 (1998).
- H. S. Cho et al., *Protein Sci.* **5**, 262 (1996).
- A. G. W. Leslie, *Crystallographic Computing* (Oxford Univ. Press, Oxford, 1990).
- Collaborative Computational Project, Number 4, *Acta Crystallogr.* **D50**, 760 (1994).
- Z. Otwinowski and W. Minor, in *Macromolecular Crystallography, Part A*, vol. 276 of *Methods in Enzymology*, C. W. Carter Jr. and R. M. Sweet, Eds. (Academic Press, San Diego, CA, 1997), pp. 307–326.
- T. C. Terwilliger and J. Berendzen, *Acta Crystallogr.* **D53**, 571 (1997); information on SOLVE is provided by T. Terwilliger (available at www.solve.lanl.gov).
- B. C. Wang, in *Diffraction Methods for Biological Macromolecules, Part B*, vol. 115 of *Methods in Enzymology*, H. W. Wyckoff, C. H. W. Hirs, S. N. Timasheff, Eds. (Academic Press, San Diego, CA, 1985), pp. 90–112.
- K. D. Cowtan and P. Main, *Acta Crystallogr.* **D52**, 43 (1996).
- T. A. Jones, J. Y. Zou, S. W. Cowan, X. Kjeldgaard, *ibid.* **A47**, 110 (1991).
- A. T. Brunger et al., *ibid.* **D54**, 905 (1998).
- E. de LaFortelle, J. J. Irwin, G. Bricogne, in *Crystallographic Computing*, P. Bourne and K. Watenpaugh, Eds., vol. 7 (available at <http://lagrange.mrc-lmb.cam.ac.uk/papers/index.html#SHARP>).
- P. J. Kraulis, *J. Appl. Crystallogr.* **24**, 946 (1991); E. A. Merritt and D. J. Bacon, *Macromolecular Crystallography, Part B*, vol. 277 of *Methods in Enzymology*, C. W. Carter Jr. and R. M. Sweet, Eds. (Academic Press, San Diego, CA, 1997), pp. 505–524.

37. We thank B. Spiller for crystallography advice, E. Abbate for construction of several HPV18 mutants, and D. S. King for mass spectrometry. We are grateful to J. Holton and other members of the Alber lab for helpful discussions; T. Alber, J. Berger, R. Stevens, and R. Tjian for suggestions and critical reading of the manuscript; L. W. Hung and T. Earnest of the Advanced Light Source (ALS) for

sharing counsel and resources; and H. Bellamy of the Stanford Synchrotron Radiation Laboratory (SSRL). The ALS facility is funded by the Office of Biological and Environmental Research of the U.S. Department of Energy (U.S. DOE), with contributions from Ernest Orlando Lawrence Berkeley National Laboratory (LBNL), Amgen, Roche, University of California at Berkeley, and Lawrence Liver-

more National Laboratory. The SSRL is funded by the U.S. DOE Office of Basic Energy Science. This work was supported by NIH grants CA30490 and CA42414 to M.R.B. X-ray coordinates are available from the authors until the data are deposited in the Protein Data Bank.

18 February 1999; accepted 19 April 1999

The Fourth Dimension of Life: Fractal Geometry and Allometric Scaling of Organisms

Geoffrey B. West,^{1,2*} James H. Brown,^{2,3} Brian J. Enquist^{2,3}

Fractal-like networks effectively endow life with an additional fourth spatial dimension. This is the origin of quarter-power scaling that is so pervasive in biology. Organisms have evolved hierarchical branching networks that terminate in size-invariant units, such as capillaries, leaves, mitochondria, and oxidase molecules. Natural selection has tended to maximize both metabolic capacity, by maximizing the scaling of exchange surface areas, and internal efficiency, by minimizing the scaling of transport distances and times. These design principles are independent of detailed dynamics and explicit models and should apply to virtually all organisms.

Evolution by natural selection is one of the few universal principles in biology. It has shaped the structural and functional design of organisms in two important ways. First, it has tended to maximize metabolic capacity, because metabolism produces the energy and materials required to sustain and reproduce life; this has been achieved by increasing surface areas where resources are exchanged with the environment. Second, it has tended to maximize internal efficiency by reducing distances over which materials are transported and hence the time required for transport. A further consequence of evolution is the incredible diversity of body sizes, which range over 21 orders of magnitude, from 10^{-13} g (microbes) to 10^8 g (whales). A fundamental problem, therefore, is how exchange surfaces and transport distances change, or scale, with body size. In particular, a longstanding question has been why metabolic rate scales as the 3/4-power of body mass, M (I).

Biological scaling can be described by the allometric equation $Y = Y_0 M^b$, where Y is a variable such as metabolic rate or life span, Y_0 is a normalization constant, and b is a scaling exponent (I). Whereas Y_0 varies with the trait and type of organism, b characteristically takes on a limited number of values, all of which are simple multiples of 1/4. For

example, diameters of tree trunks and aortas scale as $M^{3/8}$, rates of cellular metabolism and heartbeat as $M^{-1/4}$, blood circulation time and life span as $M^{1/4}$, and whole-organism metabolic rate as $M^{3/4}$. The question has been why these exponents are multiples of 1/4 rather than 1/3 as expected on the basis of conventional Euclidean geometric scaling.

Recently, we presented a model which suggested that the explanation could be found in the fractal-like architecture of the hierarchical branching vascular networks that distribute resources within organisms (2). The model accurately predicts scaling exponents that have been measured for many structural and functional features of mammalian and plant vascular systems. It is not clear, however, how this model can account for the ubiquitous 3/4-power scaling of metabolic rate in diverse kinds of organisms with their wide variety of network designs, and especially in unicellular algae and protists, which

have no obvious branched anatomy. Here we present a more general model, based on the geometry rather than hydrodynamics of hierarchical networks, that does not require the existence of such explicit structures and that can account for the pervasive quarter-power scaling in biology.

We conjecture that organisms have been selected to maximize fitness by maximizing metabolic capacity, namely, the rate at which energy and material resources are taken up from the environment and allocated to some combination of survival and reproduction. This is equivalent to maximizing the scaling of whole-organism metabolic rate, B . It follows that B is limited by the geometry and scaling behavior of the total effective surface area, a , across which nutrients and energy are exchanged with the external or internal environment. Examples include the total leaf area of plants, the area of absorptive gut or capillary surface area of animals, and the total area of mitochondrial inner membranes within cells. In general, therefore, $B \propto a$. It is important to distinguish a from the relatively smooth external surface, or "skin," enclosing many organisms. We further conjecture that natural selection has acted to maximize a subject to various constraints while maintaining a compact shape. This is equivalent to minimizing the time and resistance for delivery of resources by minimizing some characteristic length or internal linear distance of the hierarchical network.

Broadly speaking, two sets of variables can be used to describe the size and shape of an organism: a conventional Euclidean set describing the external surface, A , enclosing the total volume, V ; and a "biological" set describing the internal structure, which includes the effective exchange area, a , and the

Table 1. Examples of the biological network variables l , a , and v in plant, mammalian, and unicellular systems.

Variable	Plant	Mammal	Unicellular
l	Mean path length from root to leaf, or between leaves	Mean circulation distance from heart to capillary, or between capillaries	Mean distance from cell surface to mitochondria and between mitochondria
a	Total area of leaves; area of absorptive root surface	Total area of capillaries; gut surface area	Actual cell surface area; total surface area of mitochondrial inner membranes
v	Total wood volume; total cell volume	Total blood volume; total tissue, or cell, volume	Volume of cytoplasm

¹Theoretical Division, MS B285, Los Alamos National Laboratory, Los Alamos, NM 87545, USA. ²The Santa Fe Institute, 1399 Hyde Park Road, Santa Fe, NM 87501, USA. ³Department of Biology, University of New Mexico, Albuquerque, NM 87131, USA.

*To whom correspondence should be addressed. E-mail: gbw@lanl.gov